

1 **Original**

2 **Role of peroxisome proliferator-activated receptor- $\alpha$  in hepatobiliary**  
3 **injury induced by ammonium perfluorooctanoate in mouse liver**

4 *Mutsuko Minata*<sup>1</sup>, *Kouji H. Harada*<sup>1</sup>, *Anna Kärrman*<sup>2</sup>, *Toshiaki Hitomi*<sup>1</sup>, *Michi*  
5 *Hirosawa*<sup>1</sup>, *Mariko Murata*<sup>3</sup>, *Frank J. Gonzalez*<sup>4</sup> and *Akio Koizumi*<sup>1\*</sup>

6 From the Department of Health and Environmental Sciences, Kyoto University  
7 Graduate School of Medicine,<sup>1</sup> Kyoto, Japan 606-8501; the MTM Research Centre,  
8 Örebro University,<sup>2</sup> Örebro, Sweden 70182; Department of Environmental and  
9 Molecular Medicine, Mie University Graduate School of Medicine,<sup>3</sup> Mie, Japan  
10 514-8507; the Laboratory of Metabolism, National Cancer Institute, National Institutes  
11 of Health,<sup>4</sup> Bethesda, Maryland 20892

12 Short title: Hepatobiliary injury induced by PFOA

13 To whom correspondence: Akio Koizumi, M.D., Ph.D., Address: Department of Health  
14 and Environmental Sciences, Kyoto University Graduate School of Medicine, Kyoto,  
15 Japan 606-8501, Telephone number: 81757534456, Fax number: 81757534458, E-mail:  
16 [koizumi@pbh.med.kyoto-u.ac.jp](mailto:koizumi@pbh.med.kyoto-u.ac.jp)

17

17 Abstract

18 Peroxisome proliferator-activated receptor-  $\alpha$  (PPAR $\alpha$ ) has been suggested to protect  
19 against chemically induced hepatobiliary injuries in rodents. This function could mask  
20 the potential toxicities of Perfluorooctanoic acid (PFOA) that is an emerging  
21 environmental contaminant and a weak ligand for PPAR $\alpha$ . However the function has  
22 not been clarified. In this study, PFOA was found to elicit hepatocyte and bile duct  
23 injury in *Ppara* $\alpha$  -null mice after 4 week treatment with PFOA ammonium salt (0, 12.5,  
24 25, 50  $\mu\text{mol/kg/day}$ , gavage), suggesting that PPAR $\alpha$  protects from bile duct injury. In  
25 wild-type mice, PFOA caused major hepatocellular damage dose-dependently and  
26 minor cholangiopathy observed only at 25 and 50  $\mu\text{mol/kg}$ . In treated *Ppara* $\alpha$ -null mice,  
27 PFOA produced marked fat accumulation, severe cholangiopathy, hepatocellular  
28 damage and apoptotic cells especially in bile ducts. Oxidative stress was also increased  
29 4-fold at 50  $\mu\text{mol/kg}$  and *TNF- $\alpha$*  mRNA was upregulated more than 3-fold at 25  
30  $\mu\text{mol/kg}$  in *Ppara* $\alpha$ -null mice. Biliary bile acid/phospholipid ratios were higher in  
31 *Ppara* $\alpha$ -null mice than wild-type mice. Results from these studies suggest that PPAR $\alpha$  is  
32 protective against PFOA and have a potential role for drug induced hepatobiliary injury.

33 **Key words**

34 Peroxisome proliferator-activated receptor- $\alpha$ , Perfluorooctanoic acid, hepatobiliary  
35 injury, bile acid transporter, histopathology

36

## 36 **Introduction**

37 Peroxisome proliferator-activated receptor- $\alpha$  (PPAR $\alpha$ ) is a ligand-activated receptor  
38 that mediates critical transcriptional regulation of genes associated with lipid  
39 homeostasis. PPAR $\alpha$  is also suggested to have important roles in inflammation, immune  
40 response and hepatocarcinogenesis, however the mechanism has not been clarified.

41 Perfluorooctanoic acid (PFOA) is a fluorinated eight-carbon member of the  
42 perfluoroalkyl acid family that is amphiphilic and is used in the preparation of  
43 surfactants and fabricants <sup>1)</sup>. The potential health risk for PFOA arises from its  
44 ubiquitous distribution and persistence in the environment, and its presence in humans  
45 and wildlife<sup>2,3)</sup>. PFOA is assumed to be a weak PPAR $\alpha$  ligand because of its low degree  
46 PPAR- $\alpha$  transcriptional activations among PPAR-  $\alpha$  ligands <sup>4)</sup> and is carcinogenic to  
47 rodents <sup>5,6)</sup>.

48 The pathophysiological roles of PPAR $\alpha$  in toxicity caused by PFOA is well delineated  
49 by PPAR  $\alpha$  null mice <sup>7,8)</sup>. Rosen et al (2008) demonstrated that ablation of PPAR- $\alpha$   
50 changes profiles of transcripts related to fatty acid metabolisms, inflammation,  
51 xenobiotic metabolism and cell cycle regulation <sup>7)</sup>. Qualitative changes in transcripts


52 modified hepatotoxicity significantly in PPAR $\alpha$  null mice, leading a conclusion that  
53 PPAR $\alpha$  is required for PFOA-induced cellular alterations in mouse hepatocytes.  
54 Recently, Hays et al. demonstrated that a weak PPAR $\alpha$  ligand, bezafibrate, induces  
55 cholestasis without neoplastic changes in *Ppar $\alpha$* -null mice, and have concluded that  
56 PPAR $\alpha$  protects against potential cholestasis, while it facilitates tumor promotion <sup>9)</sup>.  
57 They have also demonstrated that a very specific PPAR $\alpha$  ligands, Wy-14,643, does not  
58 induce cholestasis <sup>9)</sup>. Thus, the toxicity profile of a chemical that up- or down-regulates  
59 via PPAR $\alpha$ -dependent and independent pathways may be modified depending on its  
60 affinity to PPAR $\alpha$  and its dose.

61 A reasonable conjecture would be that PFOA , which is known as a PPAR $\alpha$  weak  
62 ligand, might also induce cholestatic disease in PPAR $\alpha$  null mice. No study on PFOA  
63 has ever investigated so far biliary duct toxicity. This study examined whether PFOA  
64 has the potential for inducing cholestatic disease and the role of PPAR $\alpha$  has in  
65 protecting against chemical induced choestasis. We investigated whether PFOA induces  
66 cholestasis in *Ppar $\alpha$* -null mice and the dose-response relationship between PFOA and  
67 toxicological responses in PPAR $\alpha$  wild and null mice. It is well known that cholestasis  
68 is not a common response in mice, although it is a very common response to

69 xenobiotics including therapeutic drugs in human<sup>10</sup>). Thus, the null genotype of PPAR $\alpha$   
70 might reveal bile duct toxicity of many PPAR $\alpha$  inducers otherwise overlooked,  
71 although they may be recognized only at very high doses<sup>11</sup>). .

## 72 **Subjects and methods**

### 73 *Animals and treatment*

74  wild-type mice (129S4/SvImJ) and *Ppar* $\alpha$ -null mice (129S4/SvJae-*Ppar* $\alpha$ <sup>tm1Gonz/J</sup>)  
75 were originally provided from Dr. Frank J. Gonzalez (National Cancer Institute,  
76 Bethesda, MD) and housed in Kyoto University Institute of Laboratory Animals. All  
77 experiments were performed with male mice aged 8–10 weeks (22–25 g). 39 wild-type  
78 mice and 40 *Ppar* $\alpha$ -null mice were randomly assigned to four groups in accordance  
79 with the administered doses of PFOA (0, 12.5, 25, 50  $\mu$ mol/kg/day). PFOA ammonium  
80 salt (>98% purity) was purchased from Fluka Chemical (Steinheim, Switzerland) and  
81 dissolved in deionized water. Mice were treated by oral gavage (8 ml/kg) daily for 4  
82 weeks and killed by euthanasia at the end of 4 weeks, at which time, blood, liver and  
83 bile were collected.

84 Livers were weighed, and the tissue was fixed in 10% neutral-buffered  
85 formalin for light microscopic examination or 1% glutaraldehyde/1.44%  
86 paraformaldehyde solution for transmission electron microscopy for ultrastructural

87 examination. The remaining portion was flash-frozen in liquid nitrogen and stored at  
88  $-80^{\circ}\text{C}$ .

### 89 *Biochemical measurements*

90 Biochemical analyses were performed on plasma samples. These analyses were  
91 examined by Nagahama Life Science Laboratory, Oriental Yeast Co. Ltd. (Shiga, Japan)  
92 included aspartate aminotransferase (AST) and alanine aminotransferase (ALT) as  
93 hepatocellular damage markers, total bilirubin (T-Bil) and total bile acid (TBA) as  
94 cholestatic markers, and total cholesterol (T-Cho) and triglyceride (TG) as fat  
95 metabolism markers.

### 96 *Histology*

97 For light microscopy, livers were processed by routine paraffin sectioning and  
98 staining with hematoxylin and eosin (HE). For the determination of apoptosis, a  
99 terminal deoxynucleotidyltransferase (TdT)-mediated dUTP-biotin nick end labeling  
100 TUNEL test was performed. An Apop Tag kit (Oncor, Gaithersburg, MD) was used  
101 according to the manufacturer's recommendations.

102 For ultrastructural studies, livers were post-fixed in 1% osmium tetroxide in 0.2 M  
103 phosphate buffer, routinely dehydrated through a graded ethanol series, and embedded  
104 in Epon using the Luft method <sup>12)</sup>. Sections were cut in 80  $\mu\text{m}$  on a Leica EM UC6

105 ultramicrotome (Hitachi, Tokyo, Japan) with a diamond knife, and stained by the  
106 Reynolds method <sup>13)</sup>. The grids were examined under a Hitachi 7650 transmission  
107 electron microscope (Hitachi, Tokyo, Japan).

#### 108 *Analysis of PFOA*

109           Determination of PFOA in whole blood, bile and liver was performed using a  
110 modification of a method originally developed by Yline et al <sup>14)</sup>. Diluted blood, bile or  
111 homogenized liver was combined with 10 µl of a 1 µg/ml solution of <sup>13</sup>C<sub>2</sub>-PFOA as an  
112 internal standard. One milliliter of tetrabutylammonium (TBA) hydrogen sulfate and 2  
113 ml 0.5 M sodium carbonate buffer solution (pH adjusted to 10) were combined and  
114 vortexed, then 2 ml methyl *tert*-butyl ether (MTBE) was added and vortexed. The tube  
115 was centrifuged to separate the aqueous and organic phases, and 1 ml of the MTBE  
116 layer was extracted, transferred to a glass tube, and evaporated to dryness at 38°C  
117 under a gentle stream of dry nitrogen. The residue was then re-dissolved in 100 µl of  
118 100 mM benzyl bromide acetone for 1 hour at 80°C and transferred to an autosampler  
119 vial. Extracts were analyzed using gas chromatography-mass spectrometry (Agilent  
120 6890GC/5973MSD, Agilent Technologies Japan, Ltd., Tokyo, Japan) in electron impact  
121 ionization mode. PFOA was separated on an HP-5MS column (30 m length, 0.25 mm i.d.,  
122 0.25 µm film thickness) with a helium carrier gas. Splitless injections (2 µl) were

123 performed with the injector set at 220 °C, and the split was opened after 1.5 min. The  
124 initial oven temperature was 60 °C for 1.5 min, ramped at 15 °C min<sup>-1</sup> to 100 C°, and  
125 then at 40 °C min<sup>-1</sup> to 240 °C. Recoveries of <sup>13</sup>C<sub>2</sub> PFOA from biological samples (n=3)  
126 were 94 ± 2.6 % for blood, 97 ± 4.4 % for bile and 94.7 ± 4.9 % for liver, respectively.

### 127 *Measurement of 8-hydroxydeoxyguanosine (8-OHdG) in the liver*

128 8-OHdG/dG levels were measured as an indicator of oxidative DNA damage. The  
129 frozen livers were minced and gently homogenized in a homogenizer by 5 strokes in  
130 lysis solution (Qiagen, Tokyo, Japan), DNA was extracted from mice frozen liver using a  
131 DNA Extractor WB kit (Wako Pure Chemical Industries, Ltd., Osaka, Japan) <sup>15)</sup>. DNA  
132 was digested completely to nucleotides by combined treatment with Nuclease P1 (Wako  
133 Pure Chemical Industries, Ltd.) and alkaline phosphatase (Sigma Chemical Co., St.  
134 Louis, MO). Then the resulting deoxynucleoside mixture was injected into a high  
135 performance liquid chromatography apparatus (LC-10ADvp, Shimadzu, Kyoto, Japan)  
136 equipped with both a UV detector (SPD-10AVvp, Shimadzu) and an electrochemical  
137 detector (Coulochem model-5200-2, ESA, MA) <sup>16)</sup>. Each liver was examined in duplicate  
138 and the means were reported.

139 *Quantitative RT-PCR analysis for multidrug resistance protein 2 (Mdr2) and tumor*  
140 *necrosis factor α (TNF-α)*



141 Quantitative Real time (RT)-PCR was used to study *Mdr2* and *TNF- $\alpha$*  mRNA  
142 expression in the liver. Total RNA was extracted from the liver using RNeasy Lipid  
143 Tissue Mini Kit (Qiagen, Tokyo, Japan). Aliquots (10 ng) were amplified using  
144 QuantiTect<sup>®</sup> SYBR<sup>®</sup> Green RT-PCR (Qiagen,Tokyo, Japan). Quantification of the  
145 amplified products was performed on an ABI PRISM 7700 Sequence Detection System  
146 (Applied Biosystems Japan, Tokyo, Japan). All expression data were normalized to  
147 glyceraldehyde 3-phosphate dehydrogenase (*GAPDH*) mRNA from the same individual  
148 sample, to correct for differences in efficiency of RNA extraction and quality.

149 The following primers were used for RT-PCR: GAPDH: forward,  
150 5'-ATGGTGAAGGTCGGTGTGAA-3'; reverse,  
151 5'-GAGTGGAGTCATACTGGAAC-3', <sup>17)</sup> corresponding to GenBank accession  
152 number M32599; Mdr2: forward, 5'-ATCCTATGCACTGGCCTTCTGGT-3'; reverse,  
153 5'-GAAAGCATCAATACAGGGGGCAG-3', <sup>18)</sup> corresponding to GenBank accession  
154 number NM\_008830; TNF- $\alpha$ . forward, 5'-TCTTCTCAAATTCGAGTGACAAG-3';  
155 reverse, 5' -GAGAACCTGGGAGTAGACAAGGTA-3', (note: designed in our lab)  
156 corresponding to GenBank accession number NM\_013693.

157 *Determination of bile acid/ phospholipid ratio (BA/PL) in bile*

158 Commercially available kit was used for determination of bile acid and

159 phospholipid contents in bile (Wako Pure Chemical Industries). For bile acid  
160 determination, 0.1  $\mu$ l bile was diluted in 200  $\mu$ l double distilled H<sub>2</sub>O, that was added to  
161 500  $\mu$ l 3- $\alpha$ -hydroxysteroid dehydrogenase, incubated at 37°C for 10 minutes, added to  
162 500  $\mu$ l response fixing solution, and absorbance was read at 560 nm using a Hitachi  
163 U-2000A spectrophotometer (Hitachi, Tokyo, Japan). For phospholipid determination,  
164 0.4  $\mu$ l bile was diluted in 20  $\mu$ l double distilled H<sub>2</sub>O, that was added to 3.0 ml color  
165 reagent (Phospholipid-C Test Wako, Wako Pure Chemical Industries), incubated at  
166 37°C for 5 min, and absorbance was read at 600 nm against a color reagent blank.

#### 167 *Western blot analysis of Bsep and Mrp2*

168 Western blot analysis was carried out for quantification of the protein levels  
169 of the canalicular bile salt export pump (Bsep) and the canalicular multidrug  
170 resistance-associated protein 2 (Mrp2). Membrane protein samples mixed with sample  
171 loading buffer (15  $\mu$ g protein/lane) were loaded after heating for 10 minutes at 70°C  
172 onto a 3–8% Tris-Acetate gel. Following electrophoresis, proteins in the gel were  
173 electrotransferred to PVDF-plus membranes (Immobilon-P Transfer Membrane;  
174 Millipore) for 1 hour at 30 V at 4°C. Membranes were blocked for 1 hour at room  
175 temperature with 5% non-fat dry milk in Tris-buffered saline that contained 0.05%  
176 Tween-20 (TBS-T). Blots were then incubated for 1 hour at room temperature with

177 the primary polyclonal antibody of rabbit Bsep, which was kindly provided by Rexue  
178 Wang, (British Columbia Cancer Research Center, Vancouver, BC, Canada) and rat  
179 Mrp2, which was kindly provided by Bruno Stieger (University Hospital, Zurich,  
180 Switzerland). GAPDH antibody was used as a loading control. Each primary antibody  
181 was diluted in blocking buffer (1:5000 for Bsep, 1:4000 for Mrp2, 1:1000 for  
182 GAPDH). After thorough washing, blots were incubated with donkey anti-rabbit IgG  
183 horseradish peroxidase-linked secondary antibody (1:4000 dilution with 5% non-fat  
184 milk in TBS-T) for 1 hour. Immunoreactive bands were detected with an enhanced  
185 chemical luminescence (ECL) kit (Immobilon Western; Millipore). Bsep and Mrp2  
186 proteins were visualized by exposure to Fuji Medical X-Ray film (FUJIFILM Medical  
187 Co., Ltd, Tokyo, Japan).

#### 188 *Statistical analysis*

189           Nine or 10 animals were studied in each group. All results were expressed as  
190 mean  $\pm$  SD. Comparisons between two groups were performed using an unpaired  
191 Student's *t* test, and Dunnett's test for dose-response experiments. Levene's test was  
192 used to assess the equality of variance. Trend test was performed using Jonckheere's

193 test.  $P < 0.05$  was considered to be statistically significant. Statistical analyses were  
194 done on SAS software (ver.8.2).

## 195 **Results and discussion**

### 196 *Body and liver weights (Table1)*

197 Body and liver weight changes after exposure to PFOA in both groups of mice are  
198 shown in Table 1. Absolute and relative liver weights (% body weight) were increased  
199 approximately three fold in wild-type or *Ppar $\alpha$* -null mice, and induction of  
200 hepatomegaly reached plateau levels in both genetic backgrounds at doses higher or  
201 equal to 12.5  $\mu\text{mol/kg}$ . These results demonstrated that PFOA induced hepatomegaly  
202 through non-PPAR $\alpha$ -mediated pathways as previously reported<sup>19)</sup>.

203

### 204 *Biochemical analysis (Table2)*

205 In wild-type mice, judging from the plasma AST and plasma ALT values, 12.5  
206 or 25  $\mu\text{mol/kg}$  PFOA caused hepatocellular damages with slight changes in T-Bil and  
207 TBA. The hepatocellular damages seemed to increase with increase in dose. Mild  
208 cholestasis was apparent at 50  $\mu\text{mol/kg}$ , at which dose, mild increases in T-Bil and TBA  
209 were observed. T-Cho was decreased after treatment with PFOA at 25 and 50  $\mu\text{mol/kg}$ .  
210 TG was increased after treatment with PFOA at 12.5 and 25  $\mu\text{mol/kg}$ , but was the same

211 level at 50 $\mu$ mol/kg.

212 In *Ppara* $\alpha$ -null mice, 12.5 or 25  $\mu$ mol/kg PFOA treatment induced mild  
213 hepatocellular damages indicated by ALT but those changes were not accompanied by  
214 elevation of T-Bil or TBA. At 50  $\mu$ mol/kg, PFOA, however, induced extensive  
215 hepatocellular damages and cholestasis simultaneously with a sharp contrast with wild  
216 cholestasis in wild mice. TG metabolism was significantly disturbed, even at 12.5  
217  $\mu$ mol/kg, while cholesterol metabolism was disturbed only at the highest dose of 50  
218  $\mu$ mol/kg.

219 Biochemical analysis suggested a significant modification of liver toxicity  
220 of PFOA by PPAR $\alpha$ . Hepatocytes were more vulnerable than bile duct cells to  
221 PFOA in wild-type mice. In contrast, ablation of PPAR $\alpha$  rendered the  
222 hepatocytes tolerable to PFOA-induced damage, at doses lower than 50  
223  $\mu$ mol/kg, while extensive hepatic and bile duct injuries occurred at 50  
224  $\mu$ mol/kg as shown in next section. In addition, metabolism of both T-Cho and  
225 TG was impaired more extensively in *Ppara* null than wild-type mice.

## 226 *Histology*

227 In PFOA wild-type mice, PFOA induced hepatocellular hypertrophy. The  
228 liver parenchyma showed dose-dependent eosinophilic cytoplasmic changes that were

229 morphologically consistent with peroxisome proliferation (Fig1 A-D). However, no fat  
230 droplets or focal necrosis were observed in control or treated mice at any doses. Bile  
231 duct epithelium showed a slight increase in thickness, which suggested that slight  
232 cholangiopathy occurred at 25 and 50  $\mu\text{mol/kg}$  (Fig. 1C, D).

233 The histological appearance in control *Ppara* $\alpha$ -null mice showed greater  
234 occurrence of microvesicular steatosis than in wild control mice (Fig. 1E). In  
235 PFOA-treated *Ppara* $\alpha$ -null mice, the hepatocytes showed not only hepatocellular  
236 hypertrophy, but also cytoplasmic vacuolation and a increase in microvesicular steatosis  
237 (Fig. 1F-H). Focal necrosis was detectable at 50  $\mu\text{mol/kg}$  (Fig. 1I). The most  
238 characteristic change was cholangiopathy. Although it was found in both wild and  
239 PPARa null mice treated with PFOA at 25 (Fig. 1 C and G) and 50  $\mu\text{mol/kg}$  (Fig.1 D  
240 and H), it was more intensive in the latter than in former(Fig. 1C, D, G, H). In particular,  
241 it was shown in *Ppara* $\alpha$ -null mice that bile ducts were surrounded by a few inflammatory  
242 cells and areas of fibrosis andbile plaque (Fig. 1H).

243 TUNEL staining demonstrated increased apoptosis in hepatic cells, hepatic  
244 arterial walls and bile-duct epithelium in wild-type mice treated with PFOA at 25 and  
245 50  $\mu\text{mol/kg}$  (Fig. 2A, B, E, F). On the other hand, in *Ppara* $\alpha$ -null mice, positive staining  
246 was observed mainly in bile duct epithelium at 25 and 50  $\mu\text{mol/kg}$  (Fig. 2C, D, G, H).

247           The ultrastructure of livers from control wild-type mice (Fig. 3A) exhibited  
248 numerous glycogen granules, normal lamellar arrangement of the rough endoplasmic  
249 reticulum (RER), a few normal dense peroxisomes and mitochondria. In contrast to  
250 control livers, treated wild-type mice (Fig. 3B-D) displayed, dose-dependent,  
251 hepatocyte hypertrophy, reduction or disappearance of glycogen granules, degranulation  
252 and disruption of the RER, nuclear vacuoles, extensive peroxisome proliferation, and  
253 slight proliferation of mitochondria. There were larger numbers and sizes of  
254 dark-staining peroxisomes and increased small, round-shaped mitochondria (Fig. 3B-D,  
255 I).

256 In control *Ppara* $\alpha$ -null mice (Fig. 3E) there were discernible amounts of small fat  
257 deposits in the cytoplasm. In treated *Ppara* $\alpha$ -null mice (Fig. 3F-H) there were  
258 dose-dependent hepatocyte hypertrophy, decreased amounts of glycogen granules,  
259 degranulation and disruption of the RER, and increased numbers of mitochondria. There  
260 is increased cytoplasmic lipid accumulation to varying extents, extensive mitochondrial  
261 changes that consisted of slight swelling, decreased matrix density and inconspicuous  
262 criste, but no peroxisome proliferation (Fig. 3F-H, J). In addition, bile duct epithelium  
263 showed degradation of cytoplasmic structure, vacuolization, and disintegration of nuclei  
264 and organelles. Severe bile duct epithelium injury was observed, with periductal

265 infiltration of fibroblasts and macrophages, and fibrosis (Fig. 3K).

266 *Pharmacokinetics of PFOA in whole blood, bile and liver (Table3)*

267 In order to investigate whether the absence of PPAR $\alpha$  changed the  
268 pharmacokinetics of PFOA, the concentration of PFOA was determined in whole blood,  
269 bile and liver after dosing for 4 weeks. The concentrations of PFOA in whole blood  
270 increased in proportion to dose, in both wild-type and *Ppara* $\alpha$ -null mice (Table 3). On  
271 the other hand, the concentrations in liver reached similar saturation levels at 12.5  
272  $\mu\text{mol/kg}$  in wild-type and *Ppara* $\alpha$ -null mice.

273 The concentrations of PFOA in bile increased with dose; it increased by 13.8  
274 times from 56.8  $\mu\text{g/ml}$  at a dose of 12.5  $\mu\text{mol/kg}$  to 784  $\mu\text{g/ml}$  at 25  $\mu\text{mol/kg}$ , and 38  
275 times to 2170  $\mu\text{g/ml}$  at a dose of 50  $\mu\text{mol/kg}$  in wild-type mice. Enhanced PFOA  
276 excretion indicate that the liver has a PFOA transport capacity from hepatocytes to  
277 bile duct that can be mediated, at least partly by PPAR $\alpha$ . In contrast, much lower  
278 increases were observed in *Ppara* $\alpha$ -null mice. PFOA concentrations increased by 3.2  
279 times from 19.6  $\mu\text{g/ml}$  at a dose of 12.5  $\mu\text{mol/kg}$  to 62.9  $\mu\text{g/ml}$  at 25  $\mu\text{mol/kg}$ , and by  
280 19.5 times to 383.0  $\mu\text{g/ml}$  at a dose of 50  $\mu\text{mol/kg}$ , demonstrating existence of capacity-  
281 limited and PPAR $\alpha$ -independent PFOA transport.

282 *8-OHdG levels in liver and quantitative RT-PCR of TNF- $\alpha$  mRNA*



283 In wild-type mice, PFOA did not elevate the levels of 8-OHdG in liver  
284 significantly at any dose (Fig. 4A). In contrast, in *Pparα*-null mice, the levels of  
285 8-OHdG tended to increase dose-dependently ( $P < 0.05$ ), which was significantly  
286 increased at 50  $\mu\text{mol/kg}$  ( $P < 0.05$ ) (Fig. 4A). PFOA did not alter the levels of *TNF-α*  
287 mRNA in wild-type mice (Fig. 4B). However, PFOA upregulated *TNF-α* mRNA  
288 significantly at doses of 25 and 50  $\mu\text{mol/kg}$  in *Pparα*-null mice ( $P < 0.01$  and  $P < 0.05$ ,  
289 respectively) (Fig. 4B).

290 These data demonstrated that ablation of PPAR $\alpha$  exacerbated oxidative  
291 damage and enhanced production of inflammatory cytokines after PFOA administration.

#### 292 *Quantitative RT-PCR for Mdr2, bile acids/ phospholipids ratio in bile*

293 We investigated three prototypical hepatobiliary transporters. Mdr2 transports  
294 biliary phospholipids from hepatocytes to bile via the canalicular phospholipid flippase,  
295 which alleviates bile acid toxicity in cholangiocytes<sup>20</sup>. Bsep transports bile acid from  
296 hepatocytes to bile via the canaliculi to keep bile acid concentrations constant in bile  
297<sup>21,22</sup>, and is resistant to canalicular damage in humans<sup>23</sup>. Mrp2 is a transporter of bile  
298 acid and is a sensitive indicator of canalicular damage<sup>24</sup>. Recently, PFOA has been  
299 reported to regulate liver transporters, organic anion transporting polypeptides (Oatps)  
300 and multidrug resistance-associated proteins responsible for uptake of bile acids (BAs)

301 and other organic compounds into liver, primarily via activation of PPAR $\alpha$ <sup>25,26</sup>. For  
302 investigating expression of Mdr2, we performed quantitative RT-PCR instead of  
303 Western blotting because the Mdr2 antibody was not specific for mouse Mdr2 (data not  
304 shown). In wild-type mice, the expression of *Mdr2* mRNA was significantly  
305 upregulated by PFOA at 12.5, 25 and 50  $\mu\text{mol/kg}$  ( $P < 0.05$ ,  $P < 0.01$  and  $P < 0.01$ ,  
306 respectively) (Fig. 4C). In *Ppar $\alpha$* -null mice, *Mdr2* mRNA was not induced by PFOA at  
307 12.5  $\mu\text{mol/kg}$ , however, it was induced significantly at 25 and 50  $\mu\text{mol/kg}$  ( $P < 0.05$  and  
308  $P < 0.01$ , respectively) (Fig. 4C). This non-PPAR $\alpha$ -mediated increase in Mdr2 may  
309 likely be attributable to the increase in bile acid at high dose<sup>27</sup>) or other nuclear  
310 receptors<sup>28</sup>). To confirm adaptive phospholipid transport, we examined the biliary bile  
311 acid to phospholipid (BA/PL) ratio (Fig. 4D). As expected, BA/PL ratio decreased  
312 significantly in a dose-dependent manner in PFOA-treated wild-type mice ( $P < 0.01$ ).  
313 However, no such significant adaptation was observed in PFOA-treated *Ppar $\alpha$* -null  
314 mice, suggesting that bile duct protective mechanism characterized by increasing  
315 phospholipid transport into bile did not work in the null mice.

#### 316 *Western blotting for Bsep and Mrp2*

317 Protein levels of Bsep were downregulated in treated wild-type mice  
318 significantly at 50  $\mu\text{mol/kg}$  ( $P < 0.01$ ). In contrast, in *Ppar $\alpha$* -null mice, protein level of

319 Bsep was increased significantly at 12.5  $\mu\text{mol/kg}$  ( $P < 0.01$ ), however decreased  
320 significantly at 50  $\mu\text{mol/kg}$  ( $P < 0.05$ ) (Fig. 5). The decreased levels of Bsep in  
321 *Ppara* $\alpha$ -null mice were very likely induced by severe injury of the hepatobiliary system  
322 and inflammation<sup>29,30</sup>). Protein levels of Mrp2 decreased in both wild-type mice and  
323 *Ppara* $\alpha$ -null mice at 50  $\mu\text{mol/kg}$  ( $P < 0.05$  for both types) (Fig. 5).

324 Bile duct transporters demonstrated that there were several PPAR $\alpha$ -mediated  
325 adaptive responses in wild-type mice to alleviate toxicity of PFOA, such as  
326 up-regulation of Mdr2 and down-regulation of Bsep. In contrast, these responses were  
327 not mobilized in concert in PFOA-treated *Ppara* $\alpha$ -null mice. Ablation of PPAR $\alpha$  made  
328 mice highly susceptible to bile duct injury. Mrp2 protein levels decreased in both  
329 wild-type and *Ppara* $\alpha$ -null mice, which might be independent to PPAR $\alpha$ .

330

331 To embark this study, we have hypothesized that PFOA is a potential toxicity for  
332 bile duct as Bezafibrate does<sup>9</sup>). As expected, PFOA was shown to induce cholestatic  
333 lesions more intensively in PPAR $\alpha$  null mice than in wild mice as demonstrated by  
334 clinical and pathological investigation. Simultaneously, we could demonstrate clear  
335 differences in dose dependent mobilization of transporters, Mdr2 and Bsep, between  
336 wild and null mice. Furthermore, there were differences in inducing 8-OHdG, TNF- $\alpha$

337 induction and BA/PL ratios in bile between wild and null mice. This is the first study to  
338 demonstrate a potential toxicity of PFOA for cholestatic disease and PPAR $\alpha$  dependent  
339 and independent responses.

340 Although hepatomegaly and increases in AST and ALT were observed in both  
341 wild-type and PPAR $\alpha$  null mice, microscopic appearance and ultrastructure of liver  
342 indicated different modes of action, including biomarkers investigated in this study.

343

344 In terms of the mechanism of bile duct injury, we focused on the changes in bile  
345 compositions and expression levels of hepatobiliary transporters. BA/PL ratio was  
346 decreased immediately in PFOA-treated wild-type mice. On the contrary it was  
347 increased at 12.5 $\mu$ mol/kg and decreased gradually at higher PFOA dose in *Ppar $\alpha$* -null  
348 mice. In wild-type mice, the decreased BA/PL ratio may protect against bile duct-injury  
349 induced by the effects of the toxic bile. Expression of *Mdr2* mRNA was clearly  
350 upregulated in all treated wild-type mice, whereas it was less upregulated in *Ppar $\alpha$* -null  
351 mice, which was consistent with BA/PL ratio in both groups of mice. The bile acid  
352 transporter, Bsep, also showed different responses between wild and null mice.  
353 Decreased Bsep levels were observed in both genetic background mice at higher doses,  
354 while *Ppar $\alpha$* -null mice showed a transient increase in Bsep protein levels at lowest dose,

355 12.5  $\mu\text{mol/kg}$ . Although the entire signal transduction for eliciting responses remains  
356 entirely unknown, several other factors such as farnesoid X receptor- $\alpha$  (FXR $\alpha$ ), which is  
357 known to downregulate Bsep<sup>31,32,33)</sup> and CAR<sup>28)</sup> may also be involved.

358 In conclusion, this study revealed the new insights that PPAR $\alpha$  is protective against  
359 cholestasis induced by the weak PPAR $\alpha$  ligand PFOA in using mouse model. PFOA  
360 mobilized adaptive processes regulated by PPAR $\alpha$ - fat metabolism by mitochondria and  
361 peroxisomes, oxidative stress, TNF- $\alpha$  and hepatobiliary transport systems. So we  
362 propose that PPAR $\alpha$  activators may induce either hepatocellular or bile duct injury,  
363 depending on their affinity to PPAR $\alpha$  and dose level. If so, cholestasis and its associated  
364 morbidities may also be taken into account for risk assessment of PFOA in humans  
365 since species differences is well characterized in PPAR $\alpha$ -associated signal transduction  
366 <sup>34)</sup>. Further studies are needed to clarify this hypothesis.

#### 367 Funding

368 This work was supported by Grants-in-Aid from the Japan Society for the Promotion of  
369 Science (grant number 19890107, 20590597, 20590600 and JSPS PE7509)

#### 370 References

- 371 1) Kissa E (2001) Fluorinated surfactants and repellents, 2nd ed. Marcel Dekker,  
372 New York.
- 373 2) Lau C, Anitole K, Hodes C, Lai D, Pfahles-Hutchens A, Seed J (2007)

- 374 Perfluoroalkyl acids: a review of monitoring and toxicological findings. *Toxicol*  
375 *Sci* **99**, 366-394
- 376 3) Harada K, Koizumi A (2009) Environmental and biological monitoring of  
377 persistent fluorinated compounds in Japan and their toxicities. *Environmental*  
378 *Health and Preventive Medicine* **14**, 7-19
- 379 4) Vanden Heuvel JP, Thompson JT, Frame SR, Gillies PJ (2006) Differential  
380 activation of nuclear receptors by perfluorinated fatty acid analogs and natural  
381 fatty acids: a comparison of human, mouse, and rat peroxisome  
382 proliferator-activated receptor-alpha, -beta, and -gamma, liver X receptor-beta,  
383 and retinoid X receptor-alpha. *Toxicol Sci* **92**, 476-489
- 384 5) Kennedy GL, Jr., Butenhoff JL, Olsen GW, O'Connor JC, Seacat AM, Perkins  
385 RG, Biegel LB, Murphy SR, Farrar DG (2004) The toxicology of  
386 perfluorooctanoate. *Crit Rev Toxicol* **34**, 351-384
- 387 6) Abdellatif AG, Preat V, Vamecq J, Nilsson R, Roberfroid M (1990) Peroxisome  
388 proliferation and modulation of rat liver carcinogenesis by  
389 2,4-dichlorophenoxyacetic acid, 2,4,5-trichlorophenoxyacetic acid,  
390 perfluorooctanoic acid and nafenopin. *Carcinogenesis* **11**, 1899-1902
- 391 7) Rosen MB, Abbott BD, Wolf DC, Corton JC, Wood CR, Schmid JE, Das KP,  
392 Zehr RD, Blair ET, Lau C (2008) Gene profiling in the livers of wild-type and  
393 PPARalpha-null mice exposed to perfluorooctanoic acid. *Toxicol Pathol* **36**,  
394 592-607
- 395 8) Wolf DC, Moore T, Abbott BD, Rosen MB, Das KP, Zehr RD, Lindstrom AB,  
396 Strynar MJ, Lau C (2008) Comparative hepatic effects of perfluorooctanoic acid  
397 and WY 14,643 in PPAR-alpha knockout and wild-type mice. *Toxicol Pathol* **36**,

- 398 632-639
- 399 9) Hays T, Rusyn I, Burns AM, Kennett MJ, Ward JM, Gonzalez FJ, Peters JM  
400 (2005) Role of peroxisome proliferator-activated receptor-alpha (PPARalpha) in  
401 bezafibrate-induced hepatocarcinogenesis and cholestasis. *Carcinogenesis* **26**,  
402 219-227
- 403 10) Velayudham LS, Farrell GC (2003) Drug-induced cholestasis. *Expert Opin Drug*  
404 *Saf* **2**, 287-304
- 405 11) Bhat HK, Kanz MF, Campbell GA, Ansari GA (1991) Ninety day toxicity study  
406 of chloroacetic acids in rats. *Fundam Appl Toxicol* **17**, 240-253
- 407 12) Luft JH (1961) Improvements in epoxy resin embedding methods. *J Biophys*  
408 *Biochem Cytol* **9**, 409-414
- 409 13) Reynolds ES (1963) The use of lead citrate at high pH as an electron-opaque  
410 stain in electron microscopy. *J Cell Biol* **17**, 208-212
- 411 14) Ylinen M, Hanhijärvi H, Peura P, Rönkä O (1985) Quantitative gas  
412 chromatographic determination of perfluorooctanoic acid as the benzyl ester in  
413 plasma and urine. *Archives of Environmental Contamination and Toxicology* **14**,  
414 713-717
- 415 15) Iwai S, Murai T, Makino S, Min W, Morimura K, Mori S, Hagihara A, Seki S,  
416 Fukushima S (2007) High sensitivity of fatty liver Shionogi (FLS) mice to  
417 diethylnitrosamine hepatocarcinogenesis: comparison to C3H and C57 mice.  
418 *Cancer Lett* **246**, 115-121
- 419 16) Murata M, Kurimoto S, Kawanishi S (2006) Tyrosine-dependent oxidative DNA  
420 damage induced by carcinogenic tetranitromethane. *Chem Res Toxicol* **19**,  
421 1379-1385

- 422 17) Hirosawa M, Minata M, Harada KH, Hitomi T, Krust A, Koizumi A (2008)  
423 Ablation of estrogen receptor alpha (ERalpha) prevents upregulation of POMC  
424 by leptin and insulin. *Biochem Biophys Res Commun* **371**, 320-323
- 425 18) Wagner M, Halilbasic E, Marschall HU, Zollner G, Fickert P, Langner C,  
426 Zatloukal K, Denk H, Trauner M (2005) CAR and PXR agonists stimulate  
427 hepatic bile acid and bilirubin detoxification and elimination pathways in mice.  
428 *Hepatology* **42**, 420-430
- 429 19) Yang Q, Abedi-Valugerdi M, Xie Y, Zhao XY, Moller G, Nelson BD, DePierre  
430 JW (2002) Potent suppression of the adaptive immune response in mice upon  
431 dietary exposure to the potent peroxisome proliferator, perfluorooctanoic acid.  
432 *Int Immunopharmacol* **2**, 389-397
- 433 20) Fickert P, Fuchsbichler A, Wagner M, Zollner G, Kaser A, Tilg H, Krause R,  
434 Lammert F, Langner C, Zatloukal K, Marschall HU, Denk H, Trauner M (2004)  
435 Regurgitation of bile acids from leaky bile ducts causes sclerosing cholangitis in  
436 *Mdr2 (Abcb4) knockout mice. Gastroenterology* **127**, 261-274
- 437 21) Arefai WA, Gill RK (2007) Bile acid transporters: structure, function,  
438 regulation and pathophysiological implications. *Pharm Res* **24**, 1803-1823
- 439 22) Trauner M, Boyer JL (2003) Bile salt transporters: molecular characterization,  
440 function, and regulation. *Physiol Rev* **83**, 633-671
- 441 23) Zollner G, Fickert P, Zenz R, Fuchsbichler A, Stumptner C, Kenner L, Ferenci P,  
442 Stauber RE, Krejs GJ, Denk H, Zatloukal K, Trauner M (2001) Hepatobiliary  
443 transporter expression in percutaneous liver biopsies of patients with cholestatic  
444 liver diseases. *Hepatology* **33**, 633-646
- 445 24) Trauner M, Arrese M, Soroka CJ, Ananthanarayanan M, Koeppel TA, Schlosser



- 446 SF, Suchy FJ, Keppler D, Boyer JL (1997) The rat canalicular conjugate export  
447 pump (Mrp2) is down-regulated in intrahepatic and obstructive cholestasis.  
448 *Gastroenterology* **113**, 255-264
- 449 25) Cheng X, Klaassen CD (2008) Critical role of PPAR-alpha in perfluorooctanoic  
450 acid- and perfluorodecanoic acid-induced downregulation of Oatp uptake  
451 transporters in mouse livers. *Toxicol Sci* **106**, 37-45
- 452 26) Maher JM, Aleksunes LM, Dieter MZ, Tanaka Y, Peters JM, Manautou JE,  
453 Klaassen CD (2008) Nrf2- and PPAR alpha-mediated regulation of hepatic Mrp  
454 transporters after exposure to perfluorooctanoic acid and perfluorodecanoic acid.  
455 *Toxicol Sci* **106**, 319-328
- 456 27) Schrenk D, Gant TW, Preisegger KH, Silverman JA, Marino PA, Thorgeirsson  
457 SS (1993) Induction of multidrug resistance gene expression during cholestasis  
458 in rats and nonhuman primates. *Hepatology* **17**, 854-860
- 459 28) Rosen MB, Lee JS, Ren H, Vallanat B, Liu J, Waalkes MP, Abbott BD, Lau C,  
460 Corton JC (2008) Toxicogenomic dissection of the perfluorooctanoic acid  
461 transcript profile in mouse liver: evidence for the involvement of nuclear  
462 receptors PPAR alpha and CAR. *Toxicol Sci* **103**, 46-56
- 463 29) Hartmann G, Cheung AK, Piquette-Miller M (2002) Inflammatory cytokines, but  
464 not bile acids, regulate expression of murine hepatic anion transporters in  
465 endotoxemia. *J Pharmacol Exp Ther* **303**, 273-281
- 466 30) Green RM, Hoda F, Ward KL (2000) Molecular cloning and characterization of  
467 the murine bile salt export pump. *Gene* **241**, 117-123
- 468 31) Lu TT, Makishima M, Repa JJ, Schoonjans K, Kerr TA, Auwerx J, Mangelsdorf  
469 DJ (2000) Molecular basis for feedback regulation of bile acid synthesis by

470 nuclear receptors. *Mol Cell* **6**, 507-515

471 32) Goodwin B, Jones SA, Price RR, Watson MA, McKee DD, Moore LB, Galardi  
472 C, Wilson JG, Lewis MC, Roth ME, Maloney PR, Willson TM, Kliewer SA  
473 (2000) A regulatory cascade of the nuclear receptors FXR, SHP-1, and LRH-1  
474 represses bile acid biosynthesis. *Mol Cell* **6**, 517-526

475 33) Kok T, Bloks VW, Wolters H, Havinga R, Jansen PL, Staels B, Kuipers F (2003)  
476 Peroxisome proliferator-activated receptor alpha (PPARalpha)-mediated  
477 regulation of multidrug resistance 2 (Mdr2) expression and function in mice.  
478 *Biochem J* **369**, 539-547

479 34) Gonzalez FJ, Shah YM (2008) PPARalpha: mechanism of species differences  
480 and hepatocarcinogenesis of peroxisome proliferators. *Toxicology* **246**, 2-8

481

482

482 **Figure titles and legends**

483 **Figure 1. Effects of PFOA on the mouse liver by oral gavage for 4weeks.**

484 Hematoxylin-eosin stained sections of liver from control wild-type mice (A), wild-type  
485 mice treated with PFOA at 12.5  $\mu\text{mol/kg}$  (B), 25  $\mu\text{mol/kg}$  (C), 50  $\mu\text{mol/kg}$  (D), control  
486 *Ppar $\alpha$* -null mice (E), *Ppar $\alpha$* -null mice treated with PFOA at 12.5  $\mu\text{mol/kg}$  (F), 25  
487  $\mu\text{mol/kg}$  (G), 50  $\mu\text{mol/kg}$  (H, I). Original magnification,  $\times 200$ , (A-H)  $\times 40$  (I). Wild-type  
488 mice treated with PFOA (B-D) have diffuse hepatocyte hypertrophy with numerous  
489 eosinophilic cytoplasmic granules. Control *Ppar $\alpha$* -null mice (E) has scattered small fat  
490 vacuoles. Centrilobular fat accumulations were increased dose-independently in  
491 *Ppar $\alpha$* -null mice treated with PFOA at 12.5  $\mu\text{mol/kg}$  (F), 25  $\mu\text{mol/kg}$  (G), 50  $\mu\text{mol/kg}$   
492 (H, I). Focal necroses are scattered with fat accumulation and proliferation of bile  
493 ductules is prominent in the portal tracts in *Ppar $\alpha$* -null mice treated with PFOA at 50  
494  $\mu\text{mol/kg}$  (I). Diffuse hepatocyte hypertrophy was observed in both mouse lines treated  
495 (B-D, F-H). Bile duct epithelial thickness (arrow) was observed in both mouse lines  
496 treated at 25  $\mu\text{mol/kg}$  (C, G) and 50  $\mu\text{mol/kg}$  (D, H). Diffusely distributed, fine, fatty  
497 droplets and ground-glass appearance is showed at 12.5  $\mu\text{mol/kg}$  (F) and 25  $\mu\text{mol/kg}$   
498 (G) in *Ppar $\alpha$* -null mice. Note hyperplastic changes in the biliary duct epithelium with  
499 bile plaque (arrow head) and fibrosis (open circle) as evidenced by proliferation of bile  
500 ductules (arrow) in *Ppar $\alpha$* -null mice treated with PFOA at 50  $\mu\text{mol/kg}$  (H). cv, central  
501 vein; pv, portal vein; ha, hepatic artery; bd, bile duct; f, fat droplet; ne, necrosis.

502 **Figure 2. Distribution of apoptotic cell in liver PFOA treated by oral gavage for**  
503 **4weeks by immunohistochemistry for TUNEL.**

504 Wild-type mice treated with PFOA at 25  $\mu\text{mol/kg}$  (A, E) and 50  $\mu\text{mol/kg}$  (B, F),  
505 *Ppar $\alpha$* -null mice treated with PFOA at 25  $\mu\text{mol/kg}$  (C, G) and 50  $\mu\text{mol/kg}$  (D, H).

506 Original magnification,  $\times 100$  (A-D),  $\times 400$  (E-H) the extended a part surrounded with a  
507 square in A-D, respectively. Wild-type mice treated with PFOA at 25  $\mu\text{mol/kg}$  (A, E)  
508 and 50  $\mu\text{mol/kg}$  (B, F) show diffuse positive stains in hepatocyte, vessel wall, and bile  
509 duct epithelium (arrow). *Ppar $\alpha$* -null mice treated with PFOA at 25  $\mu\text{mol/kg}$  (C, G) and  
510 50  $\mu\text{mol/kg}$  (D, H) show positive stains mainly in bile duct epithelium (arrow head).  
511 cv, central vein; pv, portal vein; ha, hepatic artery; bd, bile duct.

512 **Figure 3. Ultrastructure of hepatocyte and bile duct epithelium cells in control and**  
513 **after treatments of wild-type mice and *Ppar $\alpha$* -null mice with PFOA by oral gavage**  
514 **for 4weeks.**

515 Hepatocytes from control wild-type mice (A), wild-type mice treated with PFOA at 12.5  
516  $\mu\text{mol/kg}$  (B), 25  $\mu\text{mol/kg}$  (C), 50  $\mu\text{mol/kg}$  (D, I), Control *Ppar $\alpha$* -null mice (E),  
517 *Ppar $\alpha$* -null mice treated with PFOA at 12.5  $\mu\text{mol/kg}$  (F), 25  $\mu\text{mol/kg}$  (G), 50  $\mu\text{mol/kg}$   
518 (H, J), Bile duct epithelial cell (BEC) of *Ppar $\alpha$* -null mice treated with PFOA at 50  
519  $\mu\text{mol/kg}$  (K).

520 Numerous glycogen granules (circle) are observed in control wild-type mice (A). The  
521 increased number and size of dark staining peroxisomes were shown in treated  
522 wild-type mice (B-D, I). Hepatocytes from control *Ppar $\alpha$* -null mice (E) are similar to  
523 control wild-type mice with fewer fat droplets (f) in cytoplasm. In contrast to controls,  
524 treated *Ppar $\alpha$* -null mice (F-H, J) also display hepatocyte hypertrophy, decreased  
525 glycogen granules, degranulation and disruption of the rough endoplasmic reticulum,  
526 and increased mitochondria in dose-dependently. The marked different points contrasts  
527 to wild-type mice treated with PFOA are increased fat droplets in cytoplasm, a few  
528 peroxisomes, and a variable size and shape of mitochondria (F-H, J). Note that  
529 peroxisomes are markedly increased and slightly enlarged in size in wild-type mice

530 treated with PFOA at 50  $\mu\text{mol/kg}$  (I), and mitochondria are pleomorphic, enlarged (\*),  
531 and disorganization of cristae (arrowhead) in *Ppar $\alpha$* -null mice treated with PFOA at 50  
532  $\mu\text{mol/kg}$  (J). BECs (K) are showed degradation of cytoplasmic structure, vacuolization,  
533 disintegration of nuclei and organelles and surrounded with fibroblasts and collagen. p,  
534 peroxisome; f, fat droplet; v, vacuole. (A-H) Bar = 4  $\mu\text{m}$ , (I, J) Bar = 1  $\mu\text{m}$ , (K) Bar =  
535 10  $\mu\text{m}$ .

536 **Figure 4. (A) Effects of PFOA on 8-hydroxydeoxyguanosine from unfractionated**  
537 **livers of wild-type and *Ppar $\alpha$* -null mice.** This figure reveals the levels of 8-OHdG tend  
538 to increase dose-dependently in *Ppar $\alpha$* -null mice (Jonckheere's test,  $P < 0.05$ ), in which  
539 the levels are increased significantly at 50  $\mu\text{mol/kg}$  ( $P < 0.05$ ).

540 **Effects of PFOA on hepatic expressions of (B) *TNF- $\alpha$*  mRNA and (C) *Mdr2***  
541 **mRNA in wild-type mice and *Ppar $\alpha$* -null mice.** (B) The expressions of *TNF- $\alpha$*  mRNA  
542 are significantly increased in *Ppar $\alpha$* -null mice treated with PFOA at 25 ( $P < 0.01$ ) and  
543 50  $\mu\text{mol/kg}$  ( $P < 0.05$ ). (C) The expressions of *Mdr2* mRNA are significantly  
544 up-regulated in wild-type mice treated with PFOA at all doses (at 12.5  $\mu\text{mol/kg}$ , 25  
545  $\mu\text{mol/kg}$  and 50  $\mu\text{mol/kg}$ ,  $P < 0.05$ ,  $P < 0.01$ , respectively). In *Ppar $\alpha$* -null mice treated  
546 with PFOA, the expressions of *Mdr2* mRNA are not induced at 12.5  $\mu\text{mol/kg}$ , however  
547 induced at 25  $\mu\text{mol/kg}$  ( $P < 0.05$ ) and 50  $\mu\text{mol/kg}$  ( $P < 0.01$ ) significantly.

548 **(D) Effects of PFOA on biliary total bile acid/phospholipid (BA/PL) ratio.**

549 Biliary BA/PL ratios show significant decrease in wild-type mice treated with PFOA  
550 dose-dependently ( $P < 0.05$ ). However, no such significant adaptation is observed in  
551 *Ppar $\alpha$* -null mice treated with PFOA. Data are presented as mean  $\pm$  SD from 9 to 10  
552 animals in each group. Trend test is Jonckheere's test. \* $P < 0.05$ , \*\* $P < 0.01$  versus  
553 control controls in each group. Log-transformation was performed for expressions of

554 *Mdr2* mRNA levels due to heteroscedasticity.

555 **Figure 5. Effects of PFOA on Hepatic Bsep and Mrp2 protein levels.**

556 Each panel represents an individual experiment. There is a significant decrease in Bsep  
557 protein level in wild-type mice treated with PFOA at 50  $\mu\text{mol/kg}$  ( $P < 0.01$ ). In  
558 *Ppar $\alpha$* -null mice treated with PFOA, the levels are increased significantly at  
559 12.5  $\mu\text{mol/kg}$  ( $P < 0.01$ ), however decreased significantly at 50  $\mu\text{mol/kg}$  ( $P <$   
560 0.05). There is a significant decrease in Mrp2 protein levels in both wild-type  
561 and *Ppar $\alpha$* -null mice treated with PFOA at 50  $\mu\text{mol/kg}$  ( $P < 0.05$ ). Control  
562 wild-type mice, w0; wild-type mice PFOA treated with 12.5  $\mu\text{mol/kg}$ , w12.5;  
563 25  $\mu\text{mol/kg}$ , w25, 50  $\mu\text{mol/kg}$ , w50; control *Ppar $\alpha$* -null mice, n0; *Ppar $\alpha$* -null  
564 mice treated with PFOA at 12.5  $\mu\text{mol/kg}$ , n12.5; 25  $\mu\text{mol/kg}$ , n25, 50  $\mu\text{mol/kg}$ ,  
565 n50. Black bars, wild-type mice; white bars, *Ppar $\alpha$* -null mice. Densitometric  
566 values are presented as mean  $\pm$  SD of 3 animals in each group. \* $P < 0.05$ , \*\* $P$   
567  $< 0.01$  versus control in each group. Trend test is Jonckheere's test.

568

569

**Table 1** Body weight and liver weight changes after exposure to PFOA in wild-type and *Ppara*-null mice

PFOA dose Levels ( $\mu\text{mol/kg}$ )	At the start of the experiment		At sacrifice after 4 week dosing				
	Gross Body weight (g)	Body weight - Liver weight (g) <sup>a</sup>	Gross Body weight (g)	Liver weight (g)	Relative liver weight (%)	Body weight - Liver weight (g)	Body weight gain excluded liver
Wild-type							
0 (n=9)	23.9 $\pm$ 1.97	23.0 $\pm$ 1.89	26.6 $\pm$ 2.13	1.0 $\pm$ 0.08	3.7 $\pm$ 0.4	25.7 $\pm$ 2.22	2.7 $\pm$ 1.36
12.5 (n=10)	23.8 $\pm$ 0.79	22.9 $\pm$ 0.76	27.5 $\pm$ 2.07	3.2 $\pm$ 0.20 ***	11.3 $\pm$ 0.6***	24.7 $\pm$ 1.98	1.8 $\pm$ 1.95
25 (n=10)	24.2 $\pm$ 1.98	23.3 $\pm$ 1.90	25.5 $\pm$ 1.94	3.3 $\pm$ 0.30 ***	12.9 $\pm$ 0.8***	22.5 $\pm$ 1.71	-0.9 $\pm$ 1.64 ***
50 (n=10)	24.5 $\pm$ 1.67	23.6 $\pm$ 1.61	23.0 $\pm$ 2.90 **	3.3 $\pm$ 0.45 ***	13.1 $\pm$ 0.9***	20.5 $\pm$ 2.50	-3.1 $\pm$ 2.09 ***
PPAR $\alpha$ <sup>(-/-)</sup>							
0 (n=10)	22.7 $\pm$ 1.53	21.6 $\pm$ 1.46	25.0 $\pm$ 1.56	1.0 $\pm$ 0.12	4.7 $\pm$ 2.1	24.1 $\pm$ 1.37	2.5 $\pm$ 0.58
12.5 (n=10)	23.2 $\pm$ 1.87	22.1 $\pm$ 1.78	27.9 $\pm$ 1.99 **	3.3 $\pm$ 0.45 ***	11.6 $\pm$ 1.7 ***	25.1 $\pm$ 1.78	3.0 $\pm$ 1.44
25 (n=10)	23.5 $\pm$ 1.54	22.4 $\pm$ 1.47	27.4 $\pm$ 0.93 *	3.4 $\pm$ 0.23 ***	11.9 $\pm$ 1.2 ***	24.5 $\pm$ 1.16	2.1 $\pm$ 1.37
50 (n=10)	23.4 $\pm$ 1.88	22.3 $\pm$ 1.80	26.4 $\pm$ 2.07	3.4 $\pm$ 0.51 ***	13.0 $\pm$ 1.6 ***	23.7 $\pm$ 2.64	1.4 $\pm$ 1.98

Note: Values are expressed as mean  $\pm$  SD

\* $P < 0.05$ , \*\* $P < 0.01$ , \*\*\* $P < 0.001$  by Dunnett's test compared with 0  $\mu\text{mol/kg}$

<sup>a</sup> Liver weight was assumed as 3.7% in wild-type and 4.7% in *Ppara*-null mice of before body weight.

**Table 2** Plasma analysis of PFOA-treated wild-type and *Ppara*-null mice

PFOA dose levels ( $\mu\text{mol/kg}$ )	AST (IU/L)		ALT (IU/L)	
	Wild-type	PPAR $\alpha^{(-/-)}$	Wild-type	PPAR $\alpha^{(-/-)}$
0 (n=9, 10)	145 $\pm$ 71.1	137 $\pm$ 25.9	26 $\pm$ 7.1	23 $\pm$ 7.2
12.5 (n=10)	175 $\pm$ 29.2	145 $\pm$ 31.5 <sup>†</sup>	176 $\pm$ 62.4 <sup>+++</sup>	136 $\pm$ 45.3 <sup>+++</sup>
25 (n=10)	265 $\pm$ 146.2 <sup>*</sup>	152 $\pm$ 20.2 <sup>†</sup>	284 $\pm$ 158.9 <sup>+++</sup>	176 $\pm$ 42.8 <sup>+++</sup>
50 (n=10)	365 $\pm$ 106.0 <sup>***</sup>	870 $\pm$ 523.5 <sup>****†</sup>	328 $\pm$ 128.9 <sup>+++</sup>	1356 $\pm$ 744 <sup>++++††</sup>
	T-Bil (mg/dl)		TBA (mmol/L)	
	Wild-type	PPAR $\alpha^{(-/-)}$	Wild-type	PPAR $\alpha^{(-/-)}$
0 (n=9, 10)	0.09 $\pm$ 0.05	0.06 $\pm$ 0.02	4.5 $\pm$ 7.2	2.4 $\pm$ 2.6
12.5 (n=10)	0.05 $\pm$ 0.01 <sup>*</sup>	0.02 $\pm$ 0.01 <sup>†††</sup>	4.5 $\pm$ 1.6	1.0 $\pm$ 0 <sup>†††</sup>
25 (n=10)	0.09 $\pm$ 0.03	0.03 $\pm$ 0.01 <sup>†††</sup>	9.0 $\pm$ 4.6	1.4 $\pm$ 0.6 <sup>††</sup>
50 (n=10)	0.15 $\pm$ 0.04 <sup>**</sup>	0.47 $\pm$ 0.39 <sup>****†</sup>	12.5 $\pm$ 9.9	34.8 $\pm$ 9.1 <sup>****††</sup>
	T-Cho (mg/dl)		TG (mg/dl)	
	Wild-type	PPAR $\alpha^{(-/-)}$	Wild-type	PPAR $\alpha^{(-/-)}$
0 (n=9, 10)	115 $\pm$ 9.7	136 $\pm$ 26.8 <sup>†††</sup>	59 $\pm$ 17.6	45 $\pm$ 17.3
12.5 (n=10)	109 $\pm$ 17.7	84 $\pm$ 21.9 <sup>****†</sup>	87 $\pm$ 15.7 <sup>**</sup>	91 $\pm$ 35.5 <sup>**</sup>
25 (n=10)	95 $\pm$ 15.4 <sup>**</sup>	87 $\pm$ 13.7 <sup>***</sup>	89 $\pm$ 28.4 <sup>**</sup>	105 $\pm$ 23.8 <sup>***</sup>



50 (n=10)

86 ± 11.6<sup>\*\*\*</sup>

226 ± 23.0<sup>\*\*\*†††</sup>

51 ± 18.4

114 ± 32.1<sup>\*\*\*†††</sup>

---

AST, aspartate aminotransferase; ALT, alanine aminotransferase; T-Bil, total bilirubin

TBA, total bile acid; T-Cho, total cholesterol; TG, triglyceride

Data are expressed as mean ± SD

\* $P < 0.05$ , \*\* $P < 0.01$ , \*\*\* $P < 0.001$  by Dunnett's test compared with 0  $\mu\text{mol/kg}$

+ $P < 0.05$ , ++ $P < 0.01$ , +++ $P < 0.001$  by Dunnett's test after log-transformation due to heteroscedasticity (Levene's test  $P < 0.05$ )

† $P < 0.05$ , †† $P < 0.01$ , ††† $P < 0.001$  by  $t$ -test compared with wild-type and *Ppara*-null mice at same PFOA-dose level

**Table 3** Whole blood, bile and liver concentrations of PFOA in wild-type and *Ppara*-null mice

PFOA dose levels ( $\mu\text{mol/kg}$ )	PFOA concentration ( $\mu\text{g/ml}$ )					
	Whole blood		Bile		Liver	
	Wild-type	PPAR $\alpha^{(-/-)}$	Wild-type	PPAR $\alpha^{(-/-)}$	Wild-type	PPAR $\alpha^{(-/-)}$
0 (n=9, 10)	nd	nd	nd	nd	nd	nd
12.5 (n=10)	20.6 $\pm$ 2.4	19.3 $\pm$ 2.2	56.8 $\pm$ 26.9	19.6 $\pm$ 2.2	181.2 $\pm$ 6.3	172.3 $\pm$ 8.9
25 (n=10)	46.9 $\pm$ 3.2	36.4 $\pm$ 2.7*	784.0 $\pm$ 137.6	62.9 $\pm$ 16.7**	198.8 $\pm$ 15.4	218.3 $\pm$ 14.5
50 (n=10)	64.2 $\pm$ 6.5	71.2 $\pm$ 8.0	2174.0 $\pm$ 322.4	383.0 $\pm$ 109.9**	211.6 $\pm$ 13.3	239.7 $\pm$ 25.0

Data are expressed as mean  $\pm$  SD.

\* $P < 0.05$ , \*\* $P < 0.01$ , \*\*\* $P < 0.001$  by *t*-test compared between wild-type and *Ppara*-null mice.

nd; not detected (less than 0.001 $\mu\text{g/ml}$ )

Fig. 1

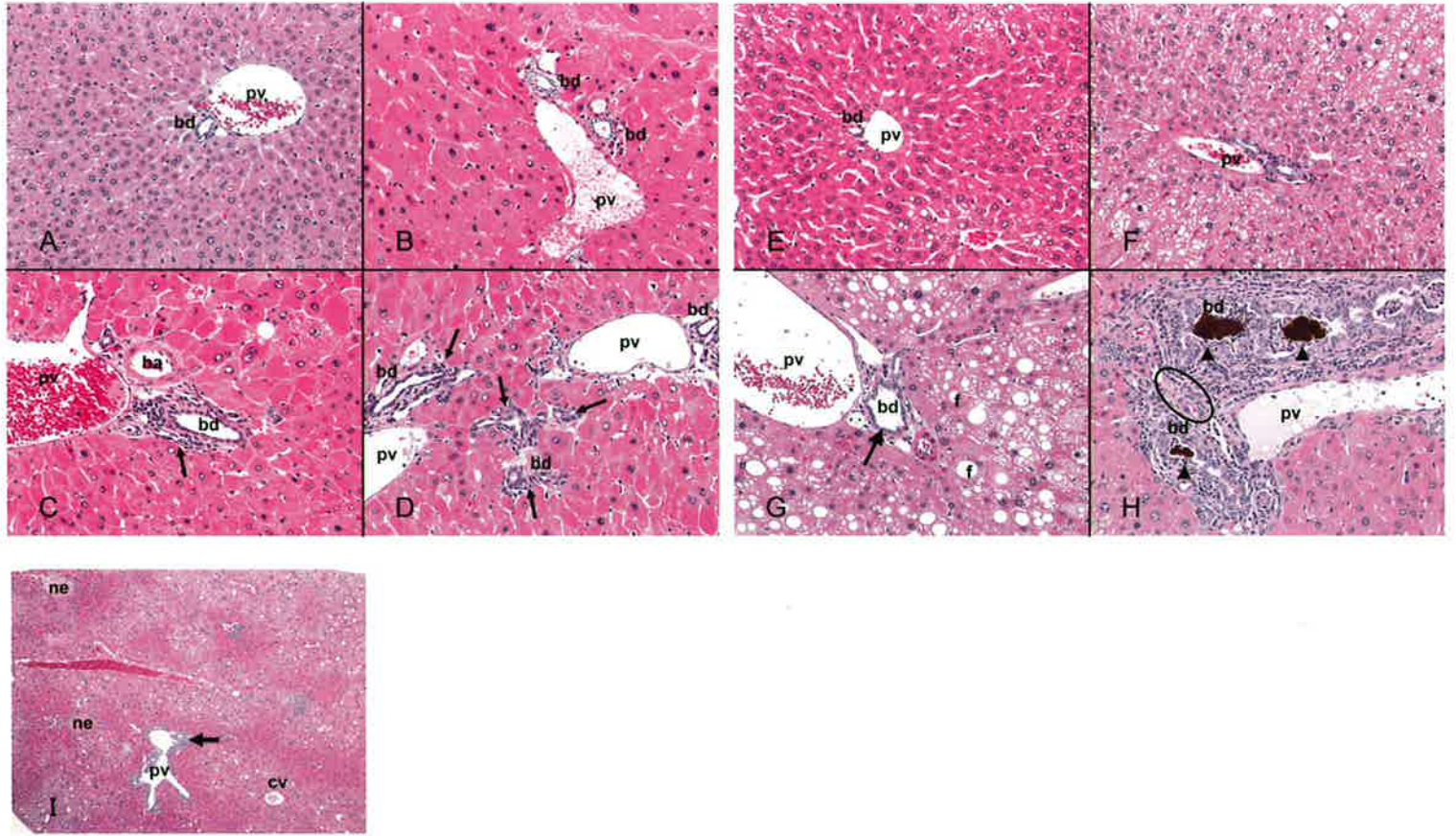


Fig. 2

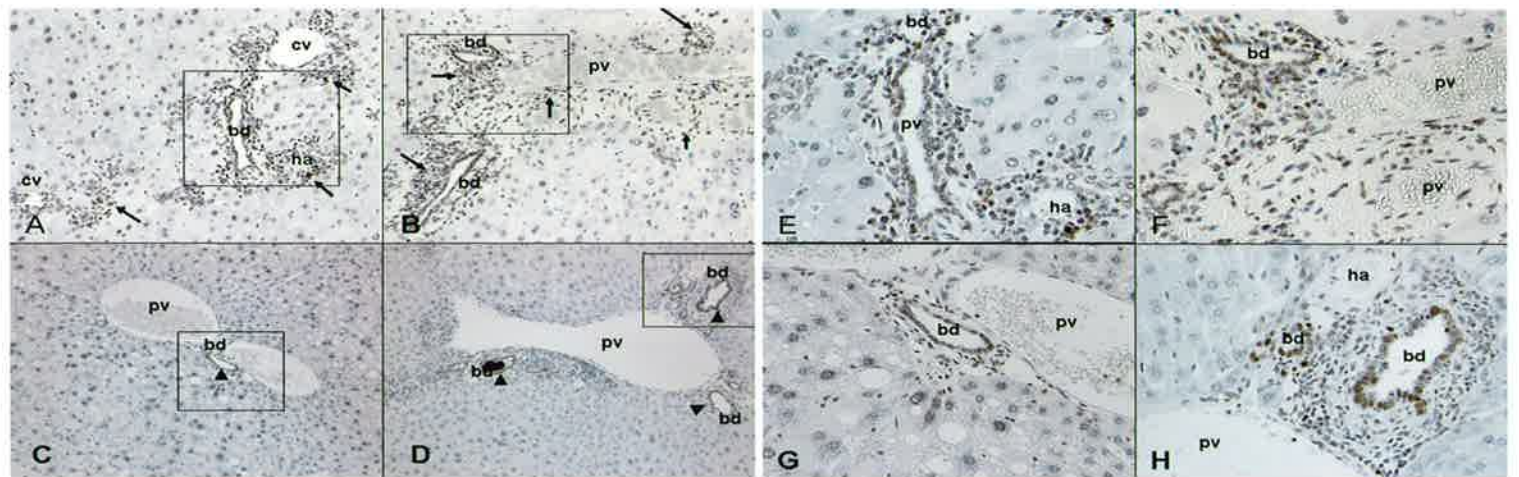


Fig. 3

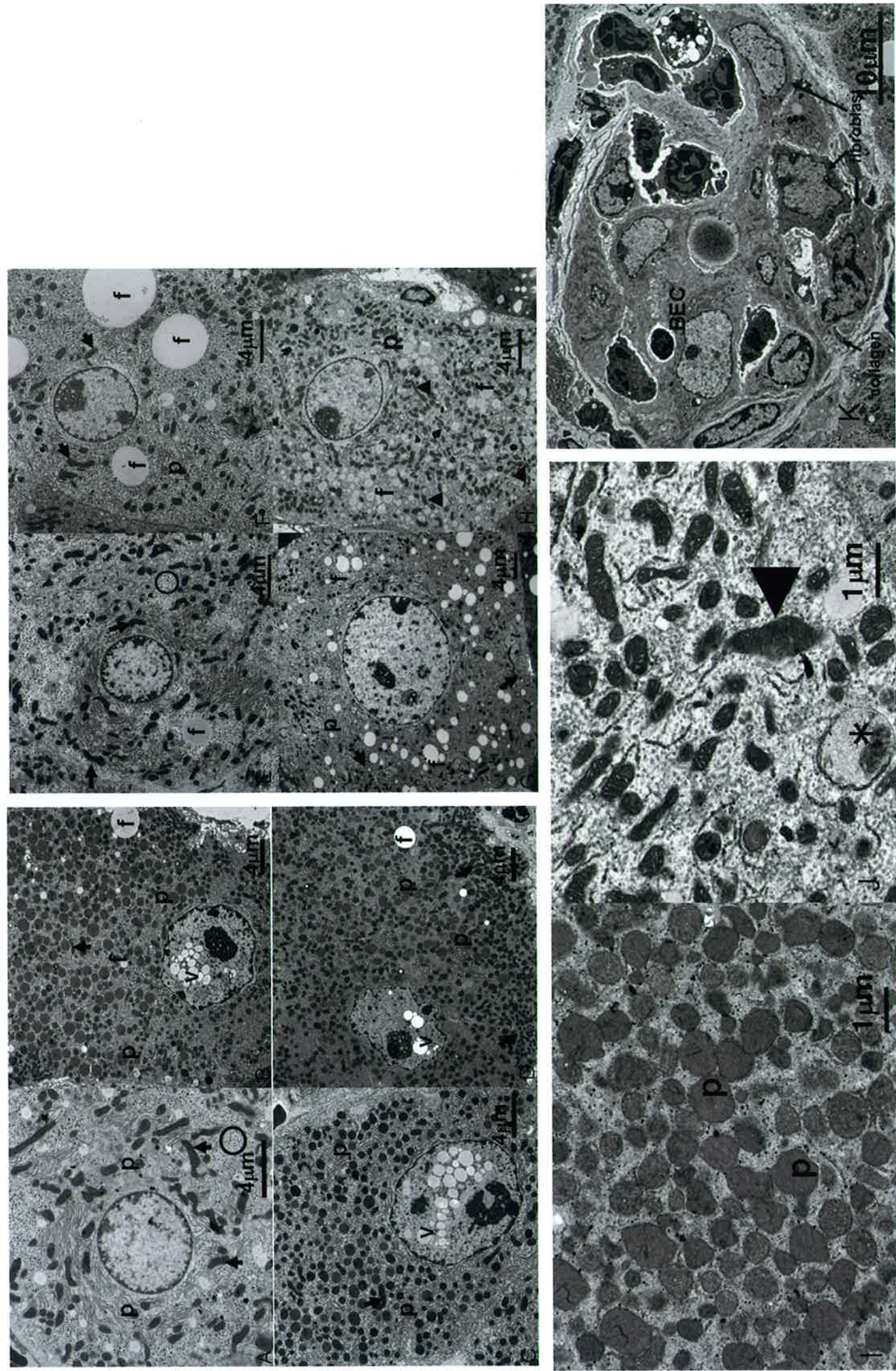


Fig. 4

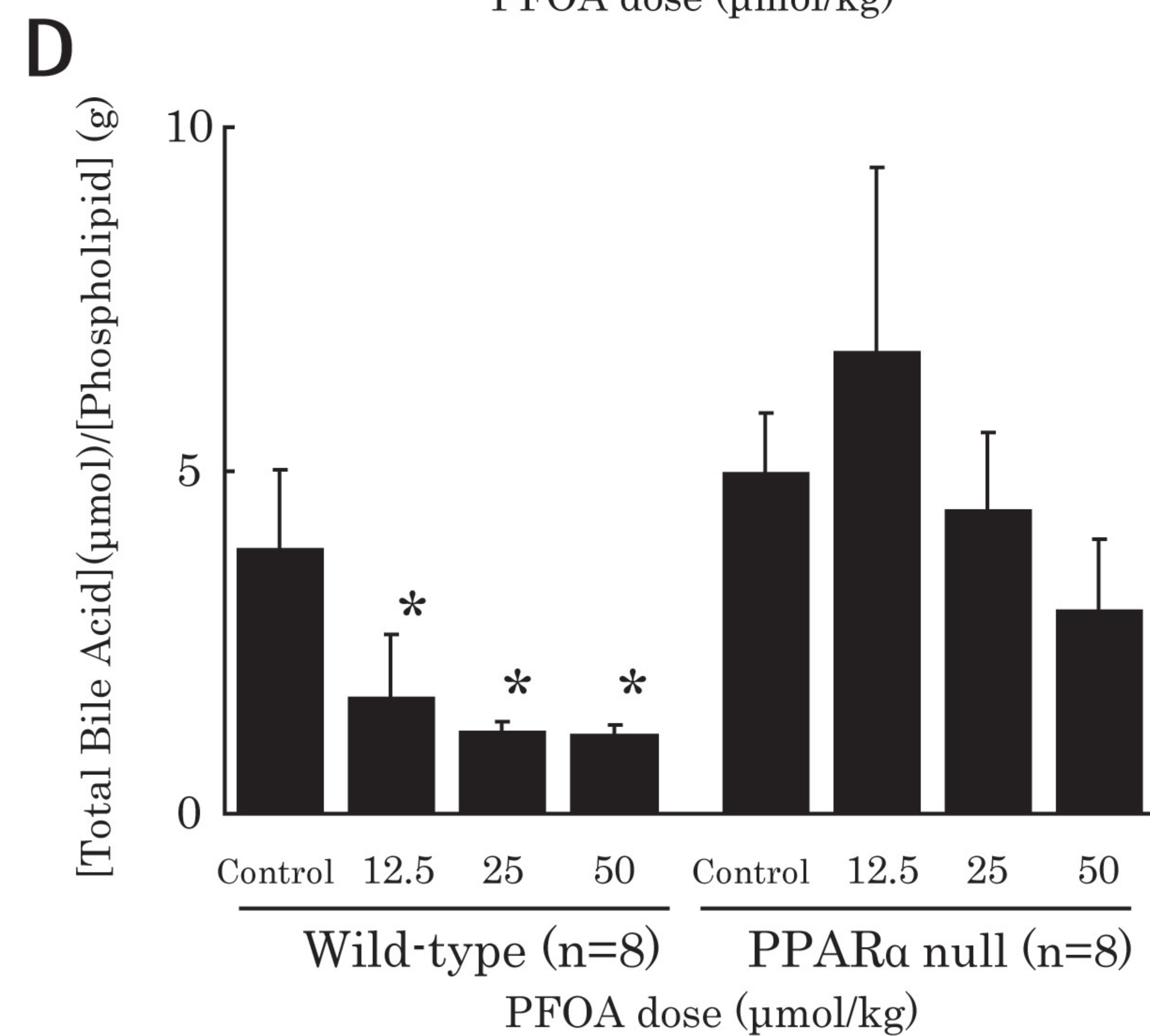
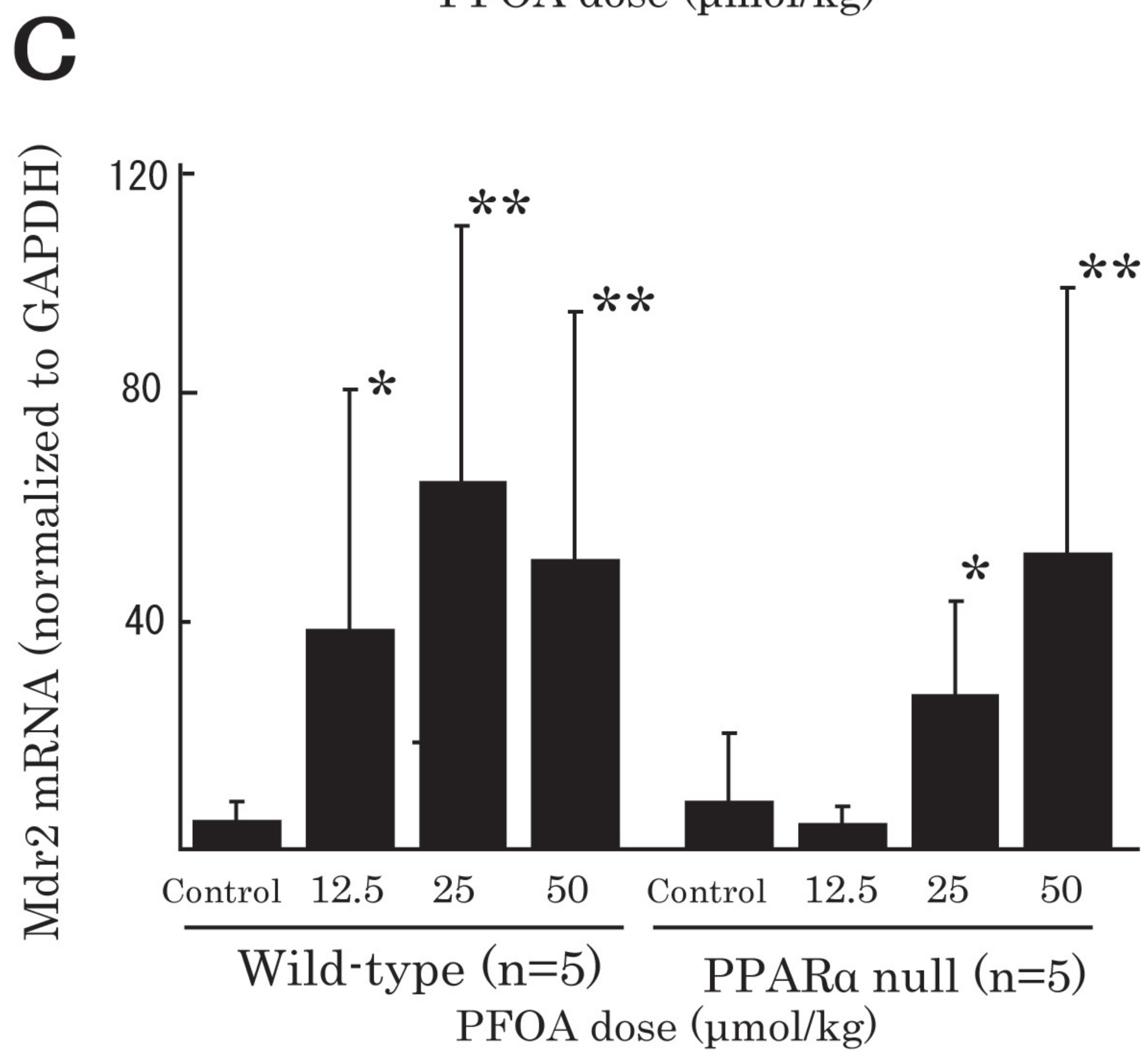
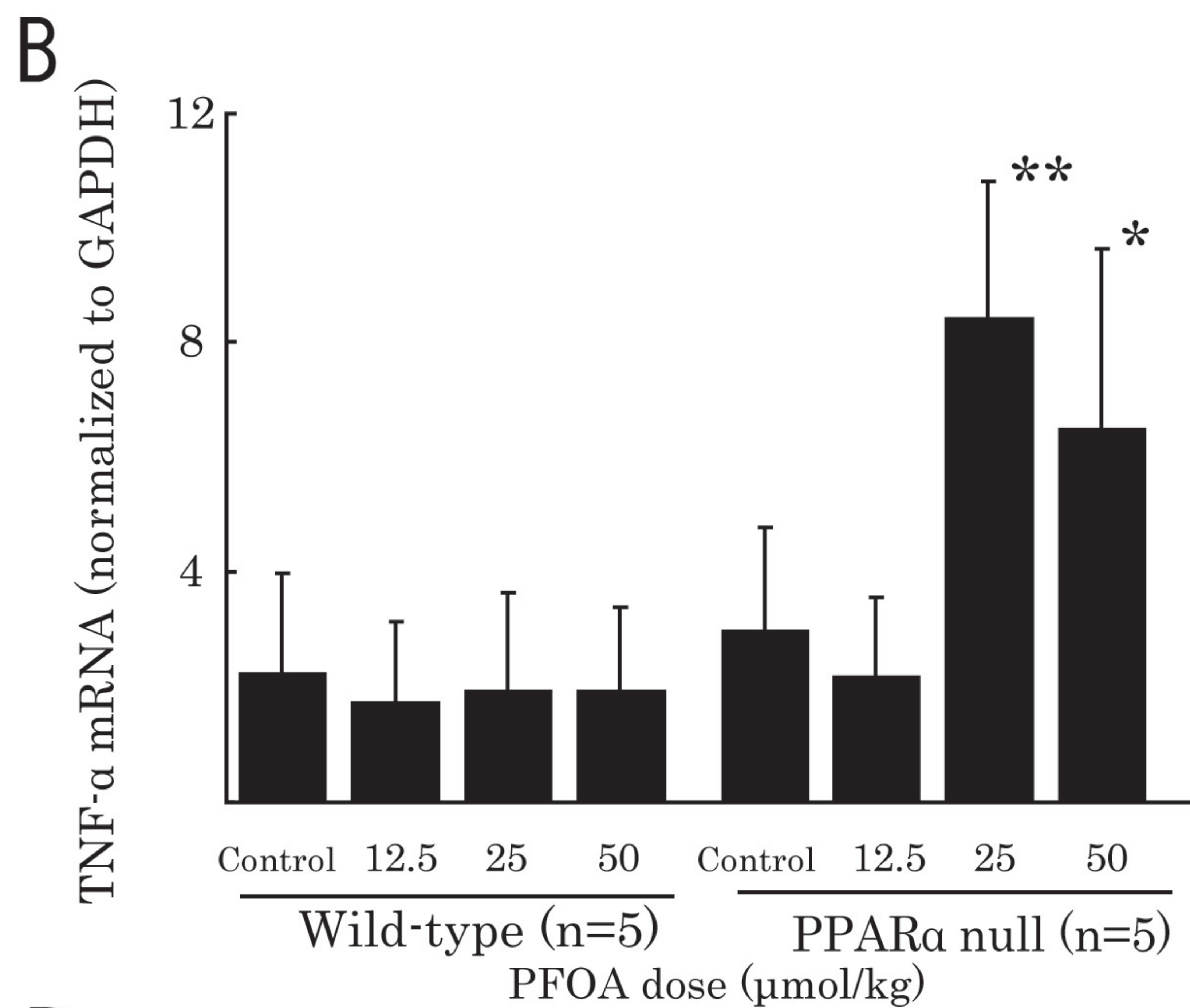
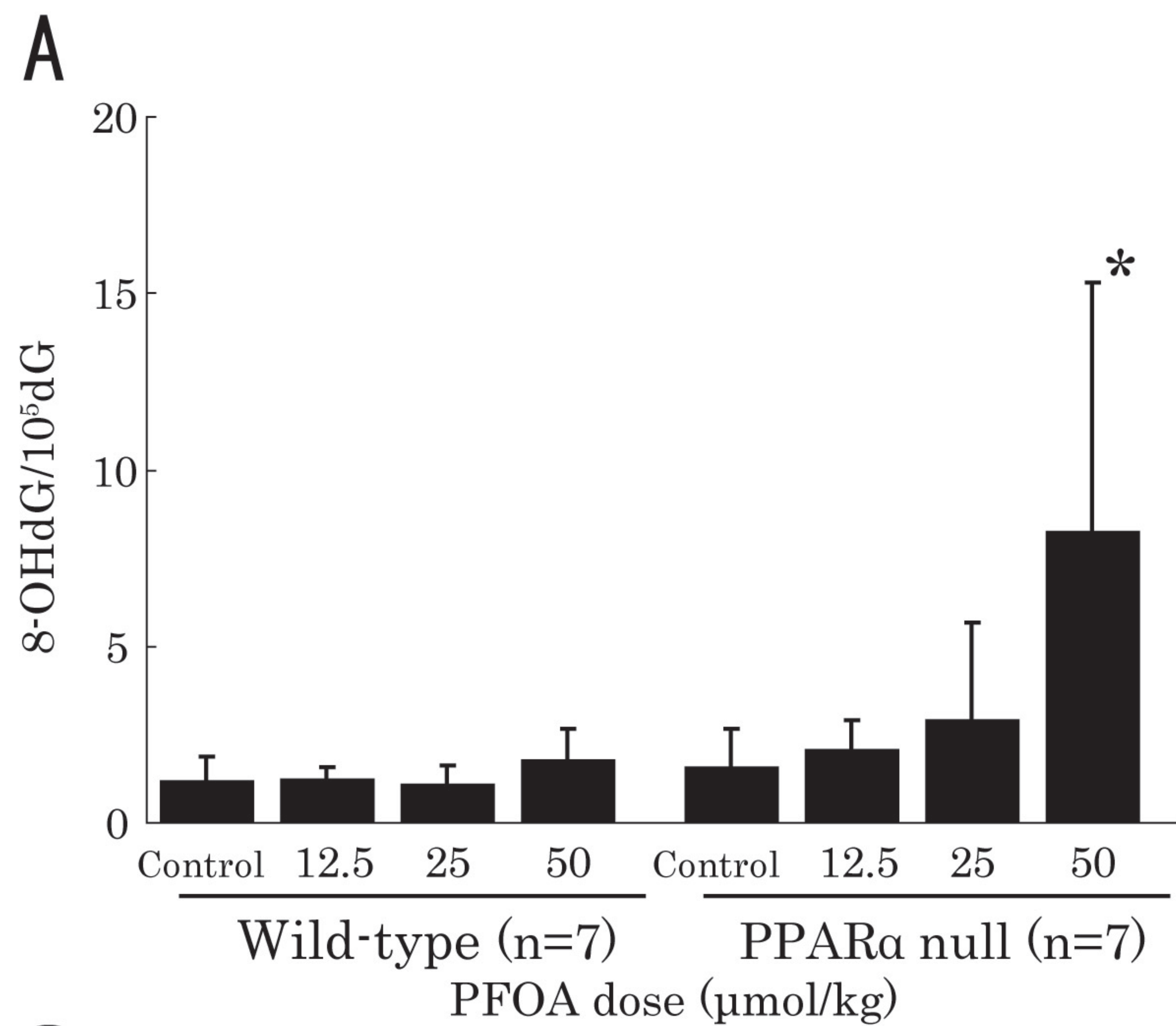
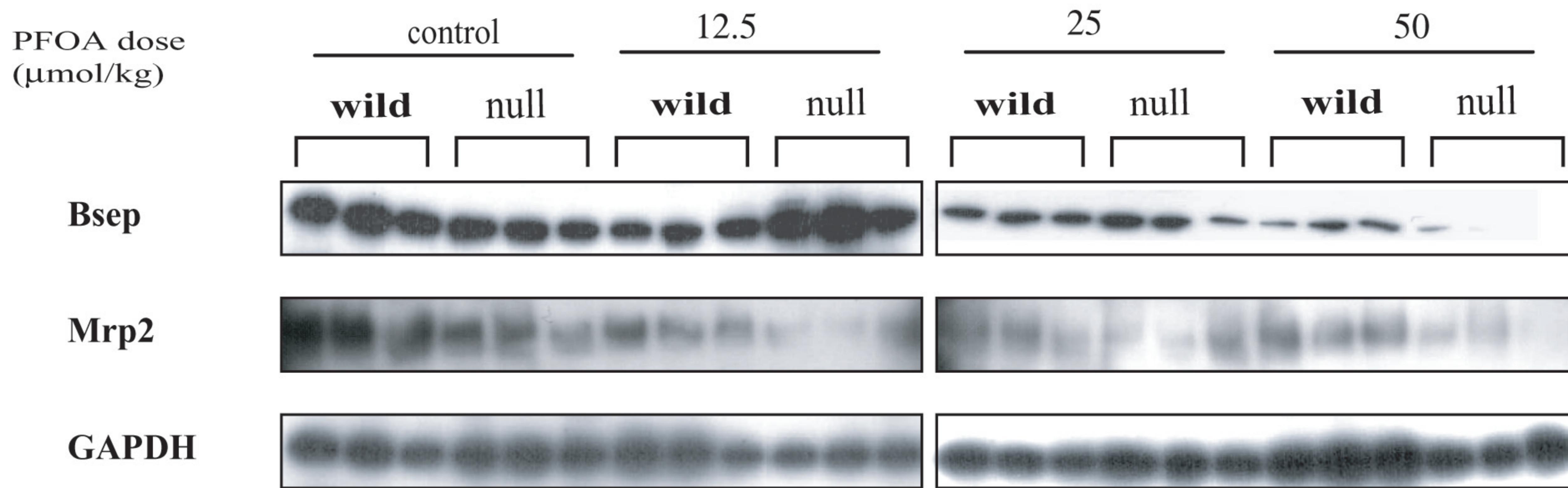


Fig. 5



Bsep/GAPDH

Mrp2/GAPDH

